Tail Region of the Primary Somatosensory Cortex and Its Relation to Pain Function

Chen-Tung Yen[1,2] and Ren-Shiang Chen[3]

Summary

In the present study, electrophysiological mapping methods were used to estimate the size of the tail representation area of the primary somatosensory cortex (SI) of the rat. Using a half-maximal evoked potential method and multiunit recording method, we estimated that the SI tail area was 0.51 and 0.78 mm^2, respectively. A dissector method was used to estimate the neuronal densities. There was, on average, 84 829 neurons/mm^3 and 117 750 neurons under 1 mm^2 of cortical area in the tail area of the SI. Therefore, there are about 94 000 neurons in the estimated 0.8 mm^2 of the SI that are involved in processing sensory signals from the tail. Anteroposteriorly oriented, evenly spaced 16-channel microwires were chronically implanted in the frontoparietooccipital cortex that was centered on the SI. Thereafter, evoked field potentials were used to estimate the change in the size of the tail area with two modalities—pain and touch—under two states: anesthetized and conscious. No significant difference was found between the size of the tail area when tactile and noxious stimulations were used. However, the number of tail responsive channels showed a significant increase when the rat was awake and behaving.

Key words Dissector method, Neuronal density, Pain, Primary somatosensory cortex, Tail

Introduction

The sensorimotor system of the rat tail has been a useful model system in pain research, such as with the tail flick test [1]. This system has many advantages to recommend as a model somatosensory system. The tail of the rat is long and

[1]Institute of Zoology, National Taiwan University, 1 Roosevelt Road, Section 4, Taipei 106, Taiwan

[2]Research Center of Brain and Oral Science, Kanagawa Dental College, Kanagawa, Japan

[3]Department of Zoology, National Taiwan University, Taipei, Taiwan

geometrically simple, and it is thus an easy target for applying specific stimuli. Second, a complete set of receptors of various somatosensory modalities, such as touch, temperature, and pain, are present in the tail. Third, because spinal roots of the tail neurons are long and thinly sheathed [2], selective activation and recording of A- or C-fibers is easier [3]. Finally, the central representation areas of the tail are relatively small [4–6], so the detailed neural circuitry of this system is easier to reach.

The somatosensory system of mammals is hierarchically organized with components in the spinal cord, medulla, thalamus, and cortex. To model any part of this system realistically, it is necessary to know each of the components involved and the fine circuitry of the intra- and interconnections. The primary somatosensory cortex (SI) is an important component in the middle of this multilayered organization. Therefore, the purpose of the present study was to estimate the number of neurons in the SI of the rat that might be involved in processing tactile and nociceptive inputs from the tail.

To obtain an estimation of total neuron number in a brain area for a given function, three sets of data are needed: the location and size of the brain area devoted to the given function and the neuronal density in this location. The tail region of the SI of the rat has been mapped many times using electrophysiological techniques [4, 6, 7]. A detailed ratunculus is shown in each article. Because these maps are composites of a great many rats, they are of little use in quantitative size estimation. The first part of the present study used unit recording and evoked field potential mapping techniques to obtain an estimate of the size of the tail area in the SI of individual rats.

In our experience, cortices that have been mapped with microelectrode penetration are swollen and distorted to varying degrees. They are usually unsuitable for morphometric measurements. The second purpose of the present study, therefore, was to find a corresponding morphological landmark for identifying the tail area of the SI in serial histological sections. This was accomplished by looking for a correspondence between the medialmost tip of layer IV (the granular layer) with the tail tip region mapped using electrophysiological recordings.

To estimate the neuronal density in the medial-tip region of the SI and adjacent areas, the dissector method [8] was used. The tail area of the SI has an estimated 117 000 neurons/mm^2, which when multiplied by the estimated size of 0.8 mm^2 gives approximately 94 000 neurons in the SI that might be involved in processing inputs from the tail.

To probe the relevance of the above data to pain processing, we used radiant laser heat pulses as a specific noxious stimulus on the tail and made recordings from the tail area of the SI in chronically instrumented rats. Our results showed that the tail area of the SI (determined by tactile stimulation while a rat was anesthetized) closely corresponded to the largest nociceptive responsive channel. The size of the nociceptive responsive area, however, greatly expanded when the rat was conscious and behaving. How this dynamically changing cortical representation pattern relates to pain function is discussed.

Original Experiments

Adult rats weighing 270–450 g were used. A preliminary survey of the innervation of the tail by gross dissection and electrophysiological mapping of the dermatome of the segmental dorsal root was undertaken. The tail of the rat is innervated by sacrococcygeal segments of the spinal cord (Fig. 1). The four sacral segmental nerves and the two coccygeal segmental nerves form a complicated caudal plexus to supply the two pairs of caudal nerves going to the tail (Fig. 2).

Three experiments were performed: (1) mapping experiments to determine the size of the tail area of the SI; (2) stereological experiments to determine the neuronal densities in the tail area of the SI; and (3) a comparison of the size of the tactile and noxious responsive areas in the tail area of the SI in anesthetized rats and in conscious, behaving rats.

Electrophysiological Mapping Experiment

Rats were anesthetized with an intraperitoneal injection of sodium pentobarbital (50 mg/kg), and the trachea, right femoral artery, and vein were cannulated. The trachea cannula was to ensure adequate ventilation. The animals breathed spontaneously during the entire recording period. The arterial blood pressure was measured through a pressure sensor connected to the arterial cannula. The venous cannula

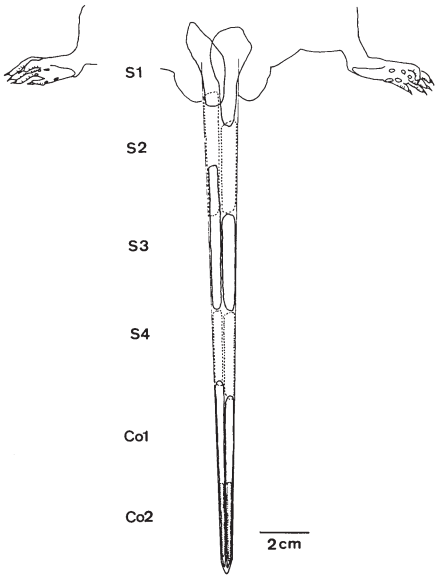

Fig. 1. Dermatome of sacrococcygeal dorsal roots determined electrophysiologically in one rat. Note that the tail base is innervated by the first sacral root (*S1*), the mid-tail by *S3* and *S4*, and the tail tip by the first coccygeal root (*Co1*) and *Co2*, respectively

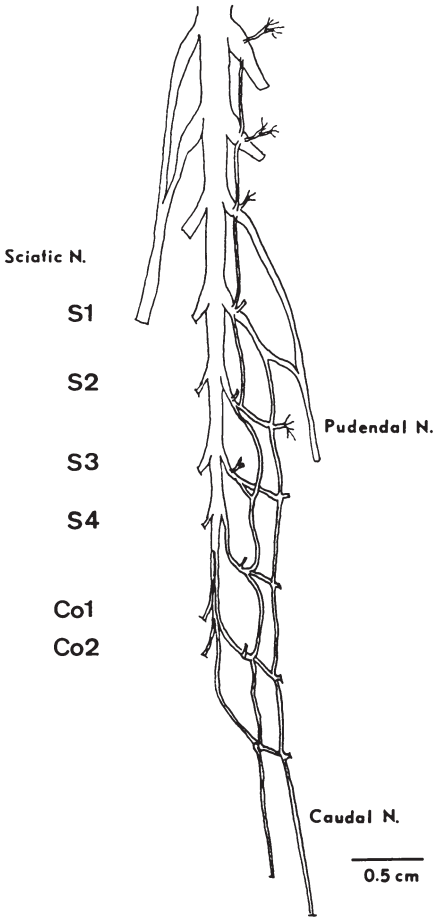

Fig. 2. Caudal plexus of one rat revealed by dissection and camera lucida tracing. Note the extensive branching of the spinal nerves. Caudal nerves going to the tail of the rat contain nerve fibers from many segmental spinal nerves

was used for supplementary doses of anesthetic. During surgery, a bolus of diluted pentobarbital was given as needed. After all surgical procedures had been completed, a continuous infusion of a diluted pentobarbital solution (10–20 mg/kg/h) was initiated at least 1 h before the actual recording began and was continued throughout the recording period. The infusion speed was adjusted to maintain a condition of areflexia with constant blood pressure and heart rate. The rectal temperature of the rat was maintained at 37.5°–37.8°C with a feedback-regulated heating blanket.

The rat was mounted on a stereotactic apparatus. A craniotomy was carried out on the right frontal and parietal bone, the dura was removed, and the surface of the cortex was covered with saline-soaked cotton balls. A vertebral clamp on the spinous process of the T1 vertebra was used to dampen the respiratory movement of the cortical surface.

Two types of mapping techniques were used: an evoked field potential technique and a unit recording technique, including single-unit and multiunit recording methods.

Evoked Potential Mapping

Field potentials evoked by electrical stimulation of the tail were used to construct topographical maps of the tail area of the SI. The stimulation electrodes consisted of three pairs of needle electrodes inserted about 5 mm deep into the tip of the tail (tail tip), in the middle portion of the tail (mid-tail), and in the place where the scales of the tail just begin to appear (tail base). The separation between the positive and negative poles was about 1 cm, with the negative pole placed rostrally.

The recording electrodes were glass micropipettes, the tip diameters of which were sharpened to 20–40 μm. These electrodes were filled with artificial cerebrospinal fluid (ACSF), which comprises NaCl 124 mmol, KCl 2 mmol, $MgCl_2$ 2 mmol, $CaCl_2$ 2 mmol, KH_2PO_4 1.25 mmol, $NaHCO_3$ 26 mmol, and glucose 11 mmol (pH 7.4) and containing 1% pontamine sky blue (K&K Laboratories, Cleveland, OH, USA). A commercial amplifier (Grass P511; AstroMed, West Warwick, RI, USA) was used to record the cortical evoked potentials (EPs) with a bandpass filter set at 3–300 Hz at a gain of 2000 or 5000. The signals were monitored with an oscilloscope and an audio monitor and were stored in a tape recorder (Neurodata DR-890). A 12-bit analog-to-digital converter card was used to digitize the cortical potential at a sampling rate of 2K online. In total, 512 peristimulus data points were collected for each stimulation cycle, and 50 cycles of cortical EPs were averaged to enhance the signal-to-noise ratio.

Stimulation parameters and recording depth were determined in a series of preliminary experiments. The recording electrode was placed in the tail area of the SI, and a constant current with a square wave pulse 2 ms in duration was used to stimulate the tail. The threshold intensities that just evoked noticeable EPs were found to be in the range of 100–200 μA, and the first component of the EP reached its maximum height at an intensity range of 300–400 μA. Subsequently, a stimulation intensity of 500 μA was used. With a repetition rate slower than once every 10 s, complex oscillatory responses were found in cortical EPs. As the interstimulus interval was shortened, the longer-latency components became smaller. The size and shape of the fast component, however, remained unchanged with a repetition rate of up to 2 Hz. Therefore, in the present study, a repetition rate of 2 Hz was chosen to emphasize the short-latency responses, which were most likely responses evoked from rapidly conducting primary afferent fibers.

A recording was made with vertical penetrations 1 mm deep in the cortex. The reasons for choosing this depth for mapping were twofold. First, this depth corresponded to the depth where most of the single-unit data were collected (see below); and second, a single large, prominent, short-latency EP was usually found at this depth following electrical stimulation of the tail.

The mapping was done sequentially with a single recording electrode in regularly spaced rectangular recording grids. The intervals between the recording points were 0.5 mm rostrocaudally and mediolaterally. Recording sequences were rostrocaudal or caudorostral rows starting either laterally or medially. At each recording point, the averaged cortical EPs were obtained for tail-base, mid-tail, and tail-tip stimulations in sequence. When a large surface blood vessel was encountered during the mapping process, this point was skipped. Data from a point farther away in the same axis was sampled instead, and the missing data point was filled in by linear interpolation. The entire process resulted in a complete set of data grids of variable dimensions, the smallest of which was 5×6, corresponding to a data collection time of 1–2 h. A representative example is shown in Fig. 3.

The stability of the cortical EPs under the conditions of the present study was tested with a control experiment. Recording electrodes of the same configuration and filled with the same filling solution were used to record cortical EPs. The electrode was placed 5 mm deep in the middle of the tail area of the SI. The exposed cortex was protected with saline-soaked cotton balls. Averaged EPs by electrical stimulation of the tail base, mid-tail, and tail tips were obtained for this point once every 0.5 h for at least 5 h. The initial latency, peak latency, and peak-to-peak amplitude of the first EP over time were compared and showed no significant changes.

The size of the tail area of the SI was estimated from isopotential maps calculated offline. An example is illustrated in Fig. 4. A 5×8 recording grid of tail stimulation-induced EP traces was obtained from sequentially recording 30 cortical points and interpolating these points. The potential changes at which a maximum EP occurred were used to construct the isopotential map. To obtain better spatial resolution, linear interpolation was used to fill in nine values between each set of adjacent data points. Two sets of gray levels were used to emphasize either the maximum amplitude of the EP or the spontaneously occurring fluctuation of the cortical potential (noise). Figure 4 shows an example of data plotted according to the maximum amplitude of the EP response. The peak amplitudes of the response in this example were 488, 408, and 288 μV, respectively, for tail-base, mid-tail, and tail-tip stimulations. These values were used as the maximum gray level, and the other levels were adjusted accordingly. A line of half-maximum amplitudes was then drawn. The area inside this line was defined as the responsive area measured with the half-maximum response amplitude. The size of the entire tail area was obtained by combining areas of the tail tip (Fig. 4c), mid-tail (Fig. 4b), and tail base (Fig. 4a) determined similarly. This is shown in Fig. 4d. Note that different cutoff levels were used for the individual maps.

Responses greater than twice the noise level were used to define the responsive area with the second method. Within each trace of the average EP, there was 20 ms of a prestimulus zone (Fig. 3). Variations of data values in this zone reflected the noise level in our preparation and the recording system. The maximal range of this variation that occurred in the prestimulus zone among all of the 30 averaged EP traces was defined as the noise level in this animal. This value was 69 μV. Therefore an isopotential line of 138 μV (i.e., twice the noise level) was drawn, and the area

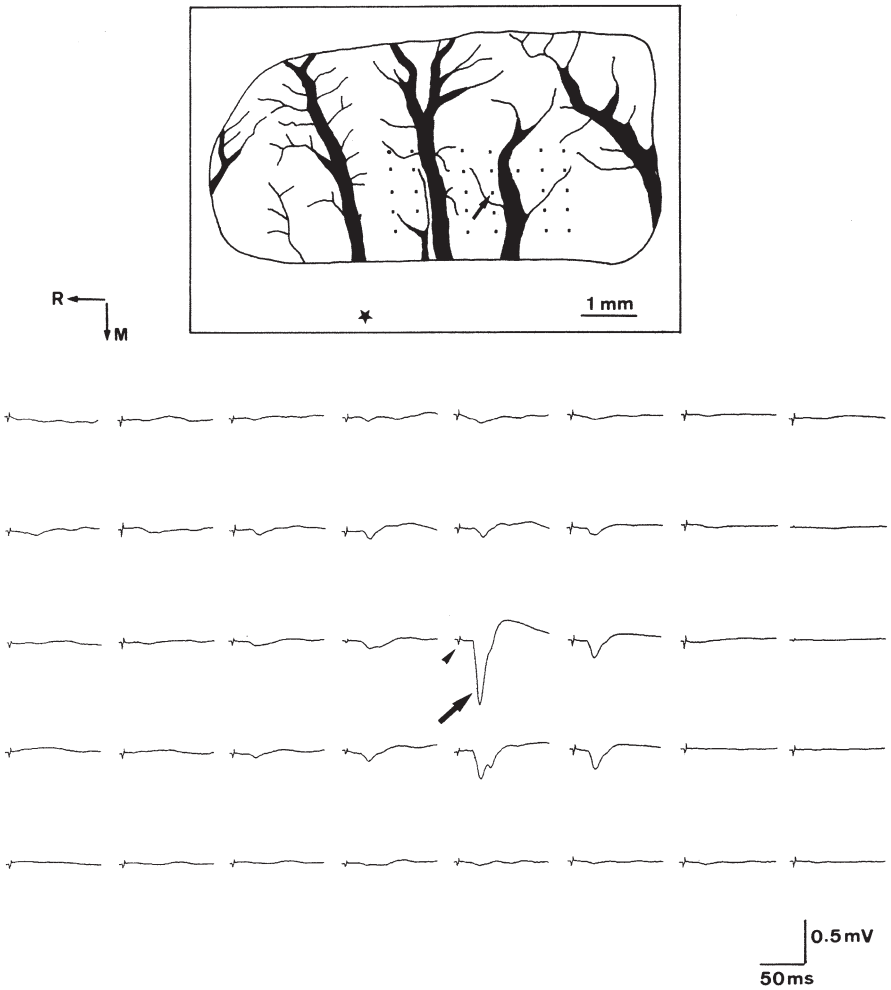

Fig. 3. Technique used for mapping the evoked field potential of the tail area of the primary somatosensory cortex (SI). **Top** Recorded points as seen from above. They comprise a 5×8 matrix in the middle of the cortical window in the contralateral frontoparietal bone. The *star* denotes the location of the bregma. **Bottom** Evoked field potential traces recorded at these points. The stimulation parameter consisted of a square wave pulse, 0.5 mA in intensity and 2 ms in width, delivered to the mid-tail of the rat at a repetition rate of 2 Hz. *Arrows* in the upper and lower panels point to the site at which the largest evoked potential was recorded in this rat. The *arrowhead* points to a stimulation artifact

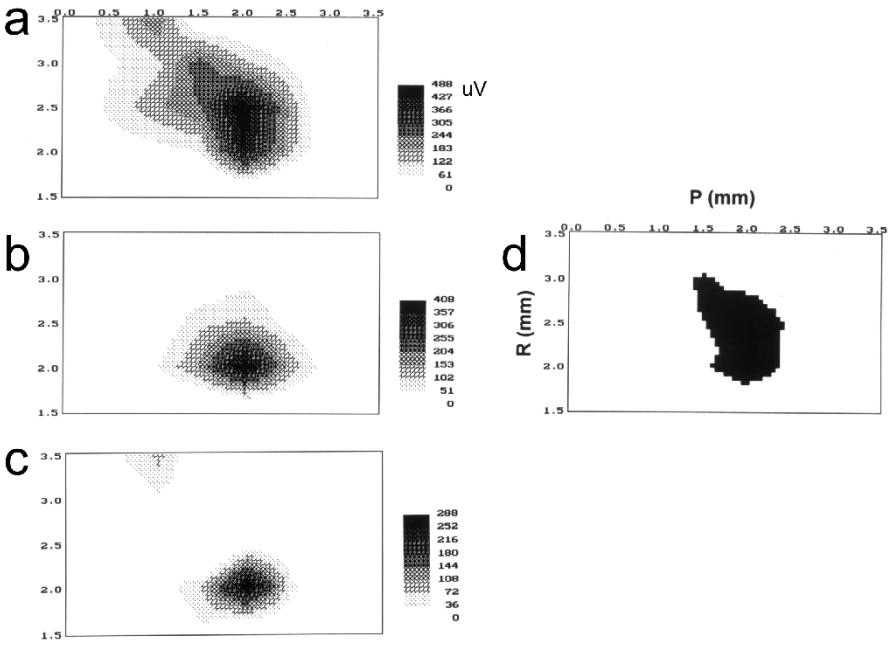

Fig. 4. Example of using the evoked cortical field potential for delineating the tail area. **a–c** Isopotential maps obtained from interpolation of cortical field potentials evoked by electrical stimulation of the tail base (**a**), mid-tail (**b**), and tail tip (**c**). **d** The tail area of this rat was determined with a combination of the three half-maximal contours

enclosed within this line was defined as the tail-base responsive area. The tail area of the rat was similarly constructed by combining the tail-base, mid-tail, and tail-tip maps.

Single-Unit and Multiunit Mapping

The preparation and recording setups used here were similar to those in the EP mapping studies. Minor modifications were made to enhance the stability. A recording chamber made of a plastic cylinder 15 mm in diameter was cemented onto the cranium with dental cement so the recorded cortical area could be covered with a layer of 4% saline agar during the recording period. A microwire sealed within a glass pipette (GL305T; MicroProbe, Clarksburg, MD, USA) was used as the recording electrode.

Multiunits could be recorded throughout the cortical depth. In contrast, stable single units were usually obtained in the deeper layers, probably corresponding to the large pyramidal cells in layer V. They were judged as single units by their all-or-none spikes.

The sequence of unit mapping was as follows. Perpendicular recording tracts began near a point 2.5 mm caudal and 2.5 mm to the right of the bregma. The response of the multiunits to cutaneous stimuli was tested at a depth of 0.9 mm. Single units were sought 0.5–1.5 mm deep in the cortex. When a clear single unit was encountered, its response to cutaneous stimuli was tested. The cutaneous stimuli used were air puffs, brushing, and light tapping. The receptive field of the multiunits was determined with a soft hairbrush. The receptive fields of single units were determined with a 10-g von Frey hair whose tip had been fire polished. The microelectrode was raised and moved 0.2–0.3 mm to another point of the cortical surface that was clear of surface vessels, and recordings began again. The sequence of recordings followed a concentric pattern surrounding the area where the receptive fields of the units covered the tail of the rat. This sequence was stopped when a full circle of nontail points had been sampled.

An example of one of the unit mapping experiments is shown in Fig. 5. The X- and Y-axes, respectively, corresponded to the anteroposterior and mediolateral

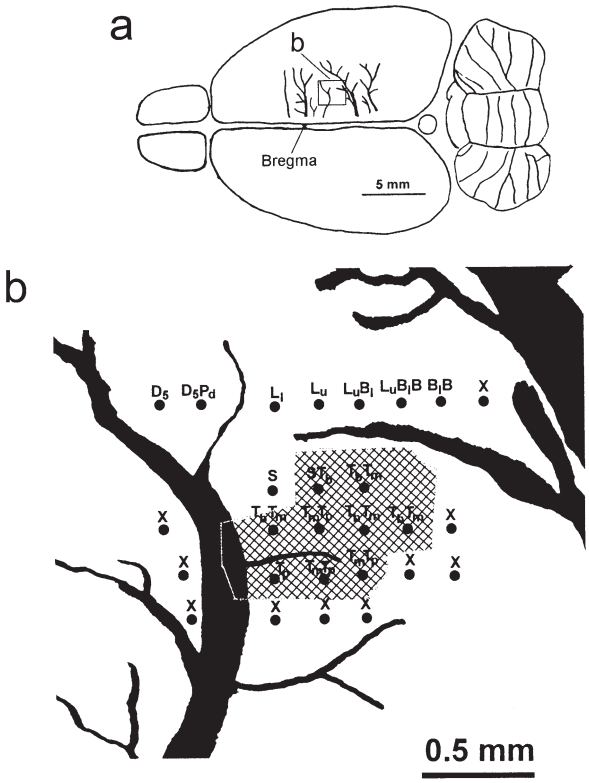

Fig. 5. Example of using the unit recording method for delineating the tail area. **a** Dorsal surface view of the brain, with the exposed vessels drawn on the right frontoparietal cortex. The *mapped area* is shown in higher magnification in **b**. Each *solid dot* represents one penetration. The tail area is *crosshatched*. *B*, back; D_5, fifth digit; L_l, lower leg; L_u: upper leg; P_d, paw pad; *S*, scrotum; T_b, tail base; T_m, mid-tail; T_p, tail tip; *X*, no receptive field found

Table 1. Estimated size of the time representative area of the primary somatosensory cortex of the rat determined by evoked field potentials or the unit recording method

	Evoked field potential		Unit recording	
Rat no.	2× Noise	1/2 Max.	Multiunit	Single unit
1	2.52	0.42		
2	2.08	0.82		
3	1.73	0.72		
4	0.38	0.08		
5			0.65	0.28
6			0.19	0.1
7			0.56	0.34
8			1.42	0.68
9			1.06	0.37
Average size	1.68	0.51	0.78	0.35

The estimated sizes are given as square millimeters

axes. The dots were the cortical points sampled. The receptive fields of the units are noted next to the recording points. Tail responsive single units were found in 9 of the 27 recording tracks. By interpolation, the tail representative area of this rat was determined as the cross-hatched area by the single-unit recording method.

The size of the tail area of the SI of the rat as estimated with the EP and unit recording methods are listed in Table 1.

Stereological Study to Determine the Neuronal Density of the SI Tail Representation Area

In the experiment to determine neuronal density of the SI tail representation area, two studies were performed. The first one used five male Wistar rats to localize the tail representative area of the SI with histological landmarks, and the second study used three rats to obtain the neuronal density in the tail representative area of the SI.

Location of the Tail Area in the SI

The correspondence of the tail area as recorded with multiunit mapping to the medial edge of the SI was determined by stereotaxically marking the recorded cortices. Multiunit mapping of the right mediorostral parietal cortex was performed as described in the mapping section. The recording electrode used here was the 20- to 40-μm tipped glass microelectrode filled with ACSF and pontamine sky blue. About 50–100 nl of the filling solution was pressure-ejected 1 mm deep into the center of the tail area by a pneumatic pump (PPM-2; Medical Systems, Great Neck, NY, USA). Within each plane, four points at equal distance occupying a square

were marked stereotactically with insect pins. These marks not only helped us align the knife angle while producing the frozen sections, they were used for calculating a shrinkage factor for the tissue.

The deeply anesthetized rat was removed from the stereotactic apparatus and perfused through the ascending aorta with buffered saline followed by a fixative composed of 4% paraformaldehyde and 0.1% glutaraldehyde in phosphate buffer. The brain was postfixed overnight and equilibrated with 30% sucrose in saline. Frozen sections of the coronal plane (50 µm thick) were cut on a sliding microtome. Camera lucida drawings of the wet tissue containing the dye marks were made with a drawing tube attached to a stereomicroscope (M3Z; WILD, Gais, Switzerland). Serial sections were mounted on gelatin-coated slides and stained with thionin (Appendix A in [9]).

The SI is characterized by a thick layer IV [10]. To test the hypothesis that the tail area is located at the medialmost tip of the SI, it was necessary to find this tip. This was done by measuring the distance between the midline and the medial edge of layer IV of the left cortex in every section. The correspondence of the center of the tail area as indicated by the dye mark was compared.

The results for five rats are shown in Fig. 6. There was a close match of the electrophysiologically determined tail tip representation area labeled with pontamine sky blue (Fig. 6, arrows) with the medialmost edge of layer IV as histologi-

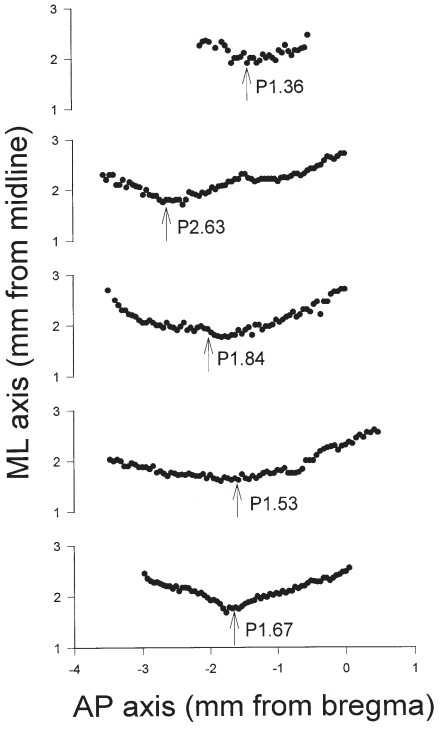

Fig. 6. Close match of the histological landmark (i.e., the medialmost edge of the layer IV boundary), with the electrophysiologically determined tail tip location (*arrows*) in five rats. The distances of the medial edge of the layer IV boundary from the midline were determined and plotted on the Y-axis for the antereoposterior (*AP*) level (X-axis) of 50-µm serially sectioned coronal sections

cally determined on the anteroposterior axis, at times with a mismatch of as small as one to two sections (<100 μm). In contrast, the points where the hind leg or trunk were mapped were both more than 500 μm away. On the other hand, the mediolateral locations of the pontamine sky blue dye marks were about 100–400 μm lateral to the edge of layer IV. Therefore, in the next experiment, we marked a 250-μm wide transitional zone here.

Stereological Determination of Neuronal Density

For optimal neuronal counting, intact, nonmapped brains were used. Rats were anesthetized with pentobarbital through an intracardial perfusion. After stereotactically marking the area with four insect pins, the brain was excised and postfixed as described above. After dehydration in an ascending ethanol series, the cortical block was embedded in paraffin. Serial 5-μm paraffin sections were cut coronally. The sections were stained with thionin [9] and mounted at 20 per slide.

A stereomicroscope equipped with a camera lucida was used to draw the contour of the sections and the position of the medialmost edge of layer IV. The sections containing the tail area of the SI of the rats was determined by the method shown in Fig. 6 and as described above. A light microscope (Vickers M41 Photoplan) equipped with a CCD camera and a video graphic printer (Sony UP-870MD) was used to observe and record the details of these histological sections. A 40× objective was used, and the final magnification as calibrated against a stage micrometer was 316× on the printed paper.

The dissector method was used to estimate the neuronal numbers [8, 11, 12]. Five equally spaced sections, each separated by 10 sections, were chosen as the dissectors. The adjacent section immediately next to these dissectors was used as the look-up section. For each pair of dissectors and the look-up section, a 750 μm wide column containing a 250-μm tail SI zone, a 250-μm transitional zone, and a 250-μm motor cortex zone (Fig. 7) from lateral to medial was photographed at 316× from the surface of the pia mater to the white matter. Prints from all five pairs of sections were reconstructed into a large montage, each about 43 cm wide and 70 cm high. The three zones and the cortical layers were marked. Neuronal nuclei were used as test objects. Only those neurons with nuclei appearing in the dissector section but not appearing in the look-up section were counted as “tops” (Fig. 8).

The area of each cortical layer (a_{dis}) in each cortical zone was measured using a digitizer. The thickness of the section (h) was calibrated to be 4.8 μm on average. The volume of each layer (V_{dis}) in the dissector section and the cortical area (A) of the sections were calculated by the following equations.

$$V_{dis} = a_{dis} \times h \tag{1}$$

and

$$A = 250 \times h \tag{2}$$

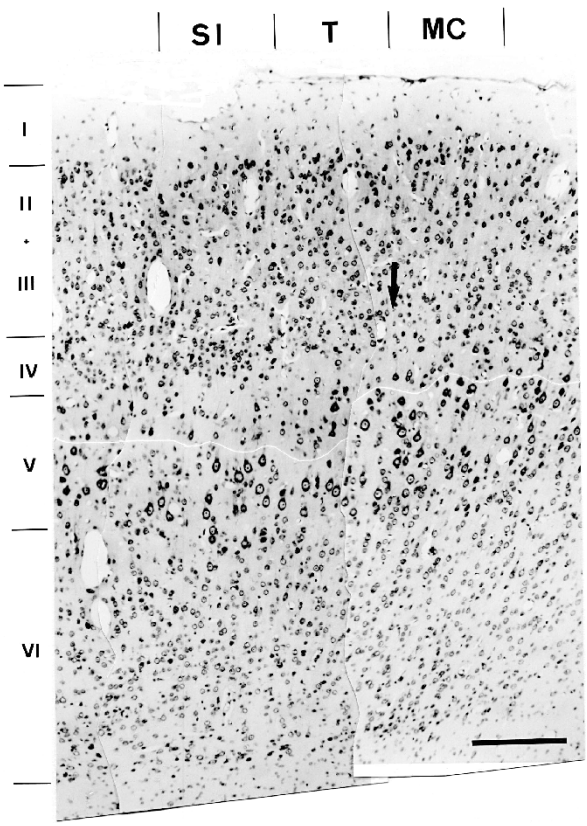

Fig. 7. Photomicrographic montage of a representative cortical section showing the use of the layer IV boundary (*arrow*) to delineate the transitional zone (*T*), the tail area of the primary somatosensory cortex (*SI*), and the motor cortex (*MC*), each of which is 250 µm in width. *Bar* 250 µm

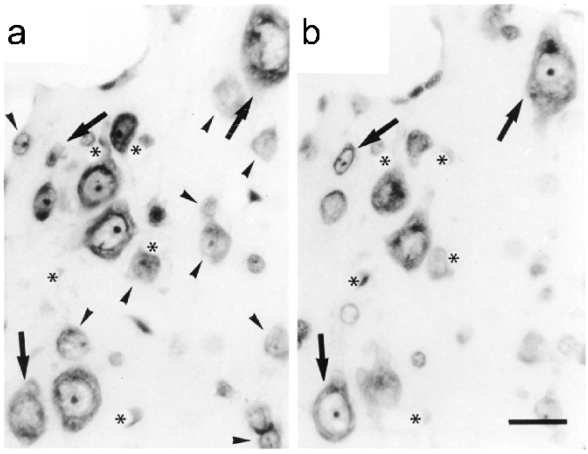

Fig. 8. Method used to determine the "tops." Vessels (*stars*) were used to align two adjacent sections. **a** Dissector section. **b** Look-up section. Those neurons that show a nucleus in the dissector section but not in the look-up section were designated "tops" (*arrowheads*). *Bar* 20 µm

Table 2. Number of neurons in the tail representative area of the primary somatosensory cortex, transition zone, and motor cortex in three rats

Cortical layer	Primary somatosensory cortex		Transition zone		Motor cortex	
	Average	SD	Average	SD	Average	SD
I	22429	4946	20159	1962	17351	2669
II/III	83083	4038	74467	1047	71892	7070
IV	170057	29701	148691	34596	—[a]	—[a]
V	70525	15350	67179	2046	69635	5689
VIA	98641	3396	95719	2292	102832	14070
VIB	100661	1618	100854	17368	98833	27669
Total	84829		78873		75729	

Results are the number of neurons per cubic millimeter
[a] There is no layer IV in the motor cortex

The number of neurons/mm^3 (Nv) and the number per 1 mm^2 of cortical area (Nc) were then calculated, respectively, as follows:

$$Nv = \frac{\sum Q_i}{\sum V_{dis}} \times 10^9 \tag{3}$$

and

$$Nc = \frac{\sum Qi}{\sum A} \times 10^6 \tag{4}$$

where Qi is the number of tops counted in each area. The numerical data were compared in each layer among the three cortical zones by repeated analysis of variance (ANOVA).

The average neuronal density was determined in three rats. The values for the volume density (Nv) are shown in Table 2, and those for the area density (Nc) are shown in Fig. 9. Our data showed that there was no significant difference among the tail region, the transitional zone, and the motor cortex. There was, on average, 84829 neurons/mm^3 and 117750 neurons per 1 mm^2 of cortical area in the tail representation region of the SI.

Comparison of the Size of the Tactile and Noxious Responsive Areas in the Tail Representative Area of the SI

The study comparing the size of the tactile and noxious responsive areas in the tail representative area of the SI was conducted on six female adult Long-Evans rats weighing 250–320 g. Surgical procedures were performed under pentobarbital anesthesia (50 mg/kg IP). Ketamine hydrochloride (50 mg/kg IM) was administered

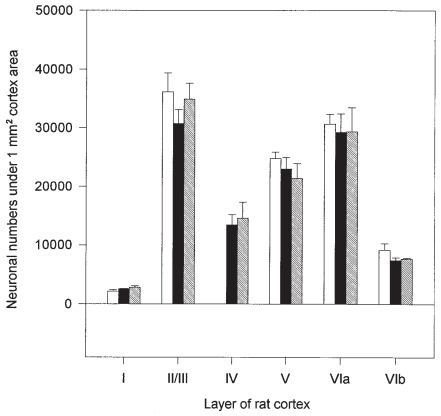

Fig. 9. Average neuronal density of the six cortical layers per 1 mm^2 of the cerebral cortex estimated for the primary somatosensory cortex (SI) (*back-slashed columns*), the transitional zone (*black columns*), and the motor cortex (*white columns*)

as necessary to maintain proper anesthetic depth so areflexia was maintained throughout the surgical period. The rat was mounted on a stereotactic apparatus. A midline incision was made over the skull. After retracting the skin and cleaning the soft tissue, small craniotomies were made for placement of intracortical microelectrodes. The microwire electrode arrays implanted in the right SI was a linear array consisting of 16 microwires aligned anteroposteriorly. Each microwire was a stainless steel wire insulated with Teflon (50 µm o.d.) [13]. The anteroposterior span of this electrode array was 8 mm and was centered on the hindlimb and tail regions of the SI. The electrode array was placed about 0.4–0.9 mm deep. The receptive fields of the individual channels were ascertained when the rat was still under anesthesia. A stainless steel screw (1 mm diameter) for recording the electroencephalogram (EEG) was placed on the left side of the skull at SI, P2.5, and L2.5 mm. The reference and ground electrodes were stainless steel screws located in the frontoparietal bones and over the top of the cerebellum (the mid-occipital bone), respectively. The hole in the skull and the implanted electrode were sealed and secured with dental cement. The rat was allowed to recover for at least 1 week after surgery.

Before the experiments, the rats were placed in the acrylic box that served as the recording chamber five times (for at least 2 h each day) to allow familiarization with the chamber. On the day of the experiments, the rats were anesthetized with halothane (4% in 100% oxygen) to connect the headstage of the amplifier to the electrodes and then remained in the recording chamber for 30 min to allow the anesthesia to wear off. The stimulus was generated by a CO_2 laser (medical surgical laser, Tjing Ling #2, National Taiwan University), with a 10.6-µm wavelength operating in the TEM_{00} mode (Gaussian distribution) [14]. Radiant heat pulses were applied to the skin of the mid-tail. The duration of the stimulation pulse was 15 ms. The beam diameter was 3 mm (unfocused). To minimize tissue damage,

sensitization, and habituation, the stimuli were randomly applied to a local skin area of the middle part of the tail 1 cm in length. The interstimulus interval was longer than 10 s. At least 20 laser heat stimulations were made for each trial, and any jerking movements of the tail (i.e., a tail flick) were noted. The output power

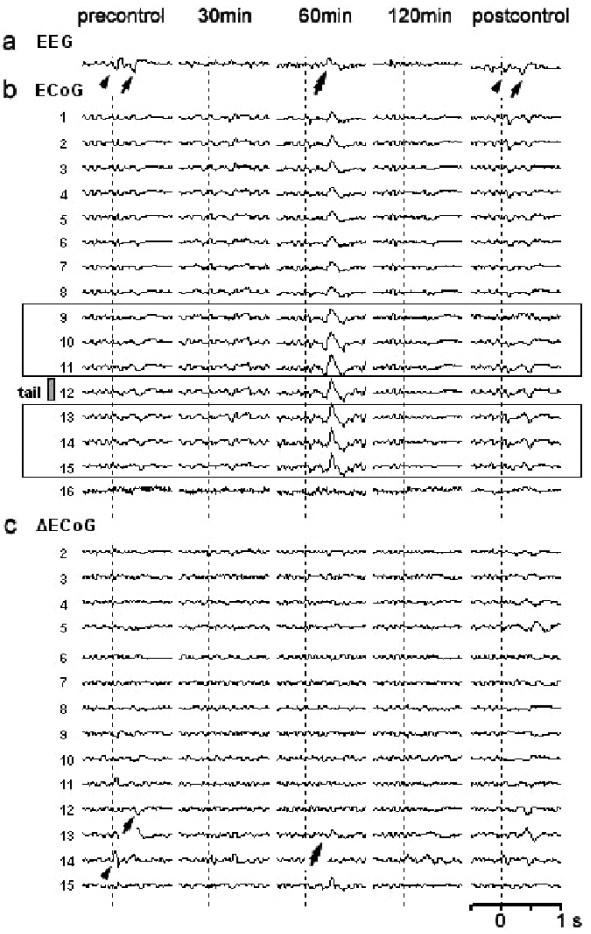

Fig. 10. Electroencephalogram (*EEG*) (*top trace*, from skull electrode) and electrocorticogram (*ECoG*) (*middle panel*, from 16-channel microwires) recorded in a chronically implanted rat. Δ*ECoG* (*lower panel*) is derived from the *ECoG* as described in the text. At the instant marked with the *vertical dotted line*, an 8-W, 15-ms CO_2 laser heat pulse was directed onto the mid-tail of the rat. Note the short-latency (*arrowhead*) and long-latency (*arrow*) responses [30, 31] in the evoked potential recorded in the consciously behaving rat either before (*precontrol*) or 24 h after (*postcontrol*) an intraperitoneal sodium pentobarbital injection (50 mg/kg). In the middle columns, evoked *EEG*, *ECoG*, and Δ*ECoG* recorded 30, 60, and 120 min after the pentobarbital injection are shown. Note that at 60 min after the injection, while the rat was still recovering from the anesthesia, the long-latency response to the noxious heat pulse returned but with reversed polarity [26, 30, 31] (*double-headed arrow*). Only channel 12 showed multiunit responses to light tactile stimulation of the mid-tail. Note the relatively larger *ECoG* responses of this channel and the channels surrounding it (*boxed channels*)

Table 3. Comparison of the size of the tactile versus noxious tail responsive area in rats chronically implanted with an anteroposteriorly oriented 16-channel linear array microwire centered on the primary somatosensory cortex

		ΔECoG, laser heat			
		Anesthetized		Conscious	
Rat no.	Multiunit, tactile—anesthetized	A[a]	C[b]	A	C
1	1	3	4	3	4
2	1	0	1	2	3
3	1	1	2	2	4
4	2	2	1	2	2
5	3	3	0	2	4
6	2	1	0	2	3
Average size	1.7	1.7	1.3	2.2	3.3*

Size is determined by the number of channels showing a response
ΔECoG, the change in the ECoG
*$P < 0.05$ vs. the anesthetized C response
[a] Short-latency primary somatosensory cortex (SI) response
[b] Long-latency SI response

was about 7–8 W. These output energies corresponded to 105–120 mJ. We examined the effect of sodium pentobarbital on the SI neural responses (50 mg/kg IP), before the pentobarbital injection (which constituted the control trial), and 30, 60, and 120 min and 24 h (postcontrol) after anesthetic administration.

The intracortical field potential (the electrocorticogram, or ECoG) and skull potentials (EEG) were recorded from the implanted microwire electrodes and screws, respectively. These neuronal activities were acquired by a multichannel neuronal acquisition processor system (MNAP; Plexon, Dallas, TX, USA). The bandpass filter used for the ECoG and EEG was 3–90 Hz. To explore a possible generator from the ECoG, the difference between adjacent channels was derived as follows. ΔECoG of channel b is:

$$\Delta\text{ECoG}(b) = 2b - (a + c) \tag{5}$$

where a and c are corresponding values of the adjacent channels.

A 16-channel microwire array was chronically implanted in six rats. Figure 10 shows a representative result of the recorded laser-heat EP and derived ΔECoG in one rat. Because the original ECoG traces of the chronically implanted electrodes might have had a common reference problem such that the evoked responses spread to all channels, we chose to use ΔECoG to estimate the size of the responsive areas. A summary is shown in Table 3. On the day of implantation, the 16-channel microwire probe was placed anteroposteriorly across a large area of the cortex that spanned anteriorly to the motor cortex, centered on the SI, and posteriorly to the occipital cortex. Individual microwires have an average interelectrode distance of 560 μm, and we found one to three tail channels (i.e., channels whose multiunit activities responded to light tapping of the mid-tail). This value did not differ significantly from the number of channels that had a short- or long-latency response to the noxious laser radiant heat applied to the mid-tail under the same anesthetic.

On the other hand, the number of responsive channels to the long-latency response was significantly greater when the rat was conscious and behaving.

Discussion

Topographically organized sensory representations exist for body parts in the cerebral cortex. Most prominent is the primary somatosensory cortex (SI). It is currently thought that inputs from the sensory epithelium during development specify and strengthen the designation of this representation [15–17]. Therefore, the relative size of the tail representation area in the SI reflects the relative number of sensory receptors compared to other body parts. On the other hand, the relative size of the SI in the total cerebral cortex is species-dependent [7, 16]. Thus, the primary cortices occupy a larger fraction of the cerebral cortex in evolutionarily simpler mammals such as rodents, whereas the association cortices dominate in advanced mammals such as primates [7, 18].

In the present study, we estimated the number of cortical neurons in the SI that are involved in processing inputs from the tail through a series of three experiments. In the first experiment, electrophysiological mapping techniques were used to delineate the size of the tail region in individual rats. The estimate ranged from 0.35 (for single-unit mapping) to 1.7 mm^2 (with the EP height twice the noise). Individually, the range was even wider, from barely detectable to >2.5 mm^2. This is surprising in light of the general view of a stable SI. Several factors may have contributed to these variations. Methodologies may be the most important factors. Single-unit and multiunit methods detect action potential spikes, whereas the evoked field potential detects the action potential and synaptic potentials, with the synaptic potential predominating. Therefore, unit recording techniques tend to miss subthreshold signals and result in underestimates. On the other hand, all electric potential signals have a volume conduction effect because neurons are embedded and bathed in a conducting solution [19]. Therefore, the size of the source of the electrical signal may be overestimated with signals barely detectable over the noise level. Hence, a reasonable estimate should be somewhere in between. A slightly larger value than the 0.78 mm^2 measured with the multiunit method may be the most accurate estimate.

The second experiment of this study used the dissector method to estimate the neuronal density in this area. Our estimate showed a range of neuronal densities similar to those in the literature [20–24]. Combining the size of the area with the neuronal densities indicated that the number of cortical neuron processing sensory inputs from the tail was 94 000. As stated earlier in the chapter, we first thought that the neuronal number might be relatively small, so the detailed circuitry of the tail center could easily be drawn. Describing a circuitry that involves 94 000 neurons is a daunting task. Therefore, a massive simplification based on the cortical layer or cortical column, or other rules, must be used.

The primary somatosensory cortex is a key area in processing many somatosensory submodalities. Among them, pain/temperature, touch/vibration, and joint/

muscle may each be considered a larger subgroup. Supposedly, the SI is involved in the discriminative aspect of all these senses. How then should these 94 000 neurons divide their jobs, as the tail of the rat possesses all three senses? Several previous studies [25–27] addressed the representation of noxious input versus tactile input in the SI area. A general consensus is that the representation area of the two submodalities overlap and are superimposed on each other in the SI. In most of those studies, it was found that nociceptive inputs activated a relatively larger area than did tactile inputs. It is unclear, however, as to whether this reflects only that noxious stimulations are usually stronger, and stronger inputs activate larger areas than do weaker ones. In the present study, we found no significant difference between the receptive channel numbers responding to light tapping versus those responding to noxious radiant heat. It may be that the crudeness of the methodology used in the present study could not detect such subtle differences. It remains an interesting question as to how a small volume of neurons in the cortex can perform so many sensory jobs.

Although orderly topography is the most impressive initial finding, following the finding by Merzenich et al. [28] that the loss of a digit changes the topography of the digit representations in the SI, cortical plasticity of the somatosensory system has since been documented in the barrel cortex, in the nipple area, of the monkey, of the rat, and many other mammalian species studied. More recently, it was demonstrated that acute reversible deafferentation triggers immediate reorganization of the cortical representation of the whiskers [29]. Plasticity and modifiability have been thoroughly established as the normal function of the cerebral cortex. What the orderly topography represents should be considered the final result shaped by evolution and the daily life of the subject, and this topography is continually modified throughout the individual's life.

References

1. D'Amour FE, Smith DL (1941) A method for determining loss of pain sensation. J Pharmacol Exp Ther 72:74–79.
2. Hebel R, Stromberg MW (1986) Anatomy and embryology of the laboratory rat. In: Nervous system. Biomed Verlag, Worthsee, Germany, p 125.
3. Jaw FS, Yen CT, Tsao HW, et al (1991) A modified "triangular pulse" stimulator for C fiber stimulation. J Neurosci Methods 37:169–172.
4. Chapin JK, Lin CS (1984) Mapping the body representation with SI cortex of anesthetized and awake rats. J Comp Neurol 229:199–213.
5. Mitchell D, Hellon RF (1977) Neuronal and behavioral responses in rats during noxious stimulation of the tail. Proc R Soc Lond B 197:169–194.
6. Welker C (1971) Microelectrode delineation of fine grain somatotopic organization of SmI cerebral neocortex in albino rat. Brain Res 26:259–275.
7. Woolsey CN (1958) Organization of somatic sensory and motor areas of the cerebral cortex. In: Harlow HF, Woolsey CN (eds) Biological and biochemical bases of behavior. University of Wisconsin Press, Madison, WI, pp 63–82.
8. Coggeshall RE (1992) A consideration of neural counting methods. Trends Neurosci 15: 9–13.

9. Swanson LW(1992) Brain maps: structure of the rat brain. Elsevier, Amsterdam.
10. Paxinos G, Watson C (2007) The rat brain in stereotaxic coordinates (6th ed). Academic, London.
11. Harding AJ, Halliday GM, Cullen K (1994) Practical considerations for the use of the optical dissector in estimating neuronal. J Neurosci Methods 51:83–89.
12. Pakkenberg B, Gundersen HJG (1989) New stereological method for obtaining unbiased efficient estimates of total nerve cell number in human brain areas. APMIS 97:677–681.
13. Tsai ML, Yen CT (2003) A simple method for fabricating horizontal and vertical microwire arrays. J Neurosci Methods 131:107–110.
14. Yen CT, Huang CH, Fu SE (1994) Surface temperature change, cortical evoked potential and pain behavior elicited by CO_2 lasers. Chin J Physiol 37:193–199.
15. Katz LC, Shatz CJ (1996) Synaptic activity and the construction of cortical circuits. Science 274:1133–1138.
16. Kaas JH (1997) Topographic maps are fundamental to sensory processing. Brain Res Bull 44:107–112.
17. Willshaw DJ, von der Malsburg C (1976) How patterned neural connections can be set up by self-organization. Proc R Soc Lond B 194:431–445.
18. Van Essen DC (2002) Surface-based atlases of cerebellar cortex in the human, macaque, and mouse. Ann N Y Acad Sci 978:468–479.
19. Oakley B, Schafer R (1978) Experimental neurobiology, a laboratory manual. University of Michigan Press, Ann Arbor, p 121.
20. Beaulieu C, Colonnier M (1983) The number of neurons in the different laminae of the binocular and monocular regions of area 17 in the cat. J Comp Neurol 217:337–344.
21. Beaulieu C, Colonnier M (1989) Number of neurons in individual laminae of areas 3B, 4γ, and 6aα of the cat cerebral cortex: a comparison with major visual areas. J Comp Neurol 279:228–234.
22. Beaulieu C (1993) Numerical date on neocortical neurons in adult rat, with special reference to the GABA population. Brain Res 609:284–292.
23. Ren JQ, Alika Y, Heizmann CW, et al (1992) Quantitative analysis of neurons and glial cells in the rat somatosensory cortex, with special reference to GABAergic neurons and parvalbumin-containing neurons. Exp Brain Res 92:1–14.
24. Schuz A, Palm G (1989) Density of neurons and synapses in the cerebral cortex of the mouse. J Comp Neurol 286:442–455.
25. Shouenborg J, Kalliomake J, Gustavsson P, et al (1986) Field potentials evoked in the rat somatosensory cortex by impulses in cutaneous Aβ- and C-fibers. Brain Res 397:86–92.
26. Shaw FZ, Chen RF, Tsao HW, et al (1999) Comparison of touch- and laser heat-evoked cortical field potentials in conscious rats. Brain Res 824:183–196.
27. Sun JJ, Yang JW, Shyu BC (2006) Current source density analysis of laser heat-evoked intra-cortical field potentials in the primary somatosensory cortex of rats. Neuroscience 140:1321–1136.
28. Merzenich MM, Nelson RJ, Stryker MP, et al (1984) Somatosensory cortical map changes following digit amputation in adult monkeys. J Comp Neurol 224:591–605.
29. Faggin BM, Nguyen KT, Nicolelis MAL (1997) Immediate and simultaneous sensory reorganization at cortical and subcortical levels of the somatosensory system. Proc Natl Acad Sci U S A 94:9428–9433.
30. Shaw FZ, Chen RF, Yen CT (2001) Dynamic changes of touch- and laser heat-evoked field potentials of primary somatosensory cortex in awake and pentobarbital-anesthetized rats. Brain Res 911:105–115.
31. Tsai ML, Kuo CC, Sun WZ, et al (2004) Differential morphine effects on short- and long-latency laser-evoked cortical responses in the rat. Pain 110:665–674.